Fast Algorithms For Josephson Junction Arrays : Bus–bars and Defects

Sujay Datta, Shantilal Das, and Deshdeep Sahdev *

Department of Physics, Indian Institute of Technology, Kanpur 208 016, INDIA

Ravi Mehrotra †

National Physical Laboratory, Dr. K. S. Krishnan Rd., New Delhi 110 012, INDIA

Subodh R. Shenoy ‡

I.C.T.P., P.O. Box 586, 34100, Trieste, Italy

(February 1, 2008)

We critically review the fast algorithms for the numerical study of two–dimensional Josephson junction arrays and develop the analogy of such systems with electrostatics. We extend these procedures to arrays with bus–bars and defects in the form of missing bonds. The role of boundaries and of the guage choice in determing the Green's function of the system is clarified. The extension of the Green's function approach to other situations is also discussed.

I. INTRODUCTION

The dynamical properties of Josephson junction arrays (JJAs) are currently the foci of several experimental and theoretical investigations [1]. These arrays can now be routinely fabricated in several sizes and geometries, and the characteristics of their junctions can be varied at will over a wide range of values [2]. A large body of high–precision experimental data has consequently become available for JJAs in the presence of external magnetic fields [3–5]. On the theoretical front, several insights into the behaviour of JJAs have come from numerical studies of the underlying equations of motion as given by the resistively- and capacitively-shunted junction (RCSJ) model using input current drives and defects, both controlled [6] and random [7]. With the size of experimental arrays increasing continuously, and with the number of interesting effects best seen only in large arrays going up in equal measure, it has become imperative to find ever more efficient algorithms for implementing the corresponding simulations, inclusive of all the experimental conditions. An example of the latter for current–driven arrays is the presence of bus-bars, through which the external current can be conveniently injected or withdrawn.

To understand the problem which these algorithms must address, we recall that in the RCSJ model, the total current, i_{ij}, (inclusive of external drives where applicable) flowing through the junction between sites i and j, is viewed as consisting of three 'channels' in parallel: superconductive, resistive (or ohmic) and capacitive. The currents in each of these channels can be expressed in terms of the phase difference, $\theta_{ij} = \theta_i - \theta_j$, across the junction. This leads to the following equation for the evolution of the latter in time:

$$\frac{C\hbar}{2e}\frac{d^2\theta_{ij}}{dt^2} + \frac{\hbar}{2eR}\frac{d\theta_{ij}}{dt} + I_c \sin\theta_{ij} = i_{ij} \tag{1}$$

Here C, R and I_c are the shunt–capacitance, shunt–resistance and critical current of the junction respectively. We note that Eq.(1) holds under assumptions of zero temperature, zero magnetic field and infinite perpendicular magnetic penetration depth. The last of these allows us to neglect self–induced magnetic fields.

Using total current conservation (TCC) at each site [8], we can write

$$\sum_{\langle ij \rangle} \beta_c \frac{d^2\theta_{ij}}{d\tau^2} + \frac{d\theta_{ij}}{d\tau} + \sin\theta_{ij} = I_i^{ext} \quad \forall i \tag{2}$$

---

*Email: ds@iitk.ernet.in

†Email: ravi@csnpl.ren.nic.in

‡On leave from *School Of Physics, Central University of Hyderabad, Hyderabad 500 134, INDIA*

where $I_i^{ext} = i_i^{ext}/I_c$ is the normalised current being fed to or extracted from the array site i (see Fig.), $\beta_c = 2eI_cR^2C/\hbar$ is the McCumber–Stewart parameter and $\tau = t(2eI_cR)/\hbar$ is the time measured in units of the characteristic period $\omega_c^{-1} = \hbar/(2eI_cR)$. The summation on j, over the nearest neighbours of i, can alternatively be expressed in terms of a multiplication by the discrete laplacian, G_0^{-1}. Eq.[2] then assumes the matrix form

$$\sum_j \left(G_0^{-1}\right)_{ij}\ddot{\theta}_j = \beta_c^{-1}[I_i^{ext} - \sum_{\langle ij \rangle}\dot{\theta}_{ij} + \sin\theta_{ij}] = -d_i \qquad (3)$$

If we set $\theta_i = x_i$ and $\dot{\theta}_i = y_i$, the complete set of dynamical equations reads $\left(G_0^{-1}\right)_{ij}\dot{y}_j = -d_i([x],[y])$ and $\dot{x}_i = y_i$. For the overdamped case, corresponding to $\beta_c = 0$, the relevant equations are

$$\sum_j \left(G_0^{-1}\right)_{ij}\dot{\theta}_j = -d_i \qquad (4)$$

where $-d_i$ is now given by $I_i^{ext} - \sum_{\langle ij \rangle}\sin\theta_{ij}$ but G_0^{-1} is, of course, the same as in Eq.(3).

It follows that for an $N_x \times N_y \equiv N$ array each integration time step of Eq.(4) has a complexity $\mathcal{O}(N^2)$. This is because at every upgradation of the N state variables, $\dot{\theta}$, in the under–, and θ, in the over–damped case, the constant $N \times N$ matrix G_0 has to be multiplied by the divergence vector $[d]$. It was first noticed by Eikmans and Himbergen [9] that the form of the G_0^{-1} is such that this multiplication can actually be carried out in $\mathcal{O}(N \ln N)$ steps. The procedure was subsequently improved upon by Dominguez et $al.$ [7] who combined the fast-fourier transformation used by Eikmans et $al.$ with the method of cyclic reduction to achieve a roughly 30% increase in speed.

It is noteworthy that these algorithms are applicable even in the presence of an external magnetic field. Indeed, the application of a field, $B_0\hat{z}$, perpendicular to the array transforms the phases θ_{ij} into the gauge-invariant combinations $\theta_{ij} + 2\pi A_{ij}$ where $A_{ij} = 1/\phi_0 \sum_i^j \vec{A} \cdot \vec{dl}$, $\vec{A}$ is the vector potential and $\phi_0 = \hbar/(2e)$ is the elementary flux quantum threading a plaquette. This transformation clearly affects only the divergence term, and leaves untouched the matrix G_0^{-1}, on whose form the algorithms are based. Similarly, white noise, which is taken into account by introducing a noise current into Eq.(3), also modifies only the divergence and hence does not affect the applicability of these algorithms. The statement continues to hold even if we grade each bond, i.e. make the R and I_c junction–dependent [10].

In this paper we extend these fast algorithms firstly to arrays with busbars and secondly to those with defects in the form of missing bonds. As has already been mentioned, busbars often form the current injection and/or extraction edges of experimental arrays. In experiments involving vortices, which are repelled by busbars, these have been used to produce collimated vortex–streets [11]. The dynamics of vortices have also been investigated with one edge shorted by a single busbar [12]. Arrays with defects have likewise arisen in a number of contexts. The breakdown of superconductive flow in current–driven arrays with linear defects, for example, has been investigated in some detail. The exploration of the multiple–vortex sector, which arises in this study, requires running on large arrays and is all but impossible without the algorithm we discuss below [13]. Defects can also be used to provide a collimated beam of vortices [14].

The paper is organised as follows. In section II, we present a simplified derivation of the Eikmans–Himbergen algorithm and interpret all the key equations in the familiar language of electrodynamics. Apart from being more transparent, our derivation clarifies the role of boundaries and the connection between the lattice and continum descriptions of the systems being studied. These insights are used in section III to generalize this algorithm to arrays with busbars. The case of single busbar forces us to resort to the technique of cyclic reduction, which we consequently discuss at this point. In section IV, we extend these algorithms to JJAs with defects, created by eliminating or adding bonds. Section V contains a summary and discussion of our results.

II. THE EIKMANS–HIMBERGEN ALGORITHM

A. Preliminaries

All efficient algorithms for the numerical integration of Eq.(4) make essential use of the properties of the discrete laplacian, G_0^{-1}. We thus begin by listing the more important properties of this matrix. From its definition (as given by Eqs. (3 and 4), it follows that G_0^{-1} specifies the connectivity between different sites. More precisely, $\left(G_0^{-1}\right)_{ij} = \left(G_0^{-1}\right)_{ji} = -1$ for $i \neq j$ (site i connected to site j) and 0 otherwise. The diagonal element $\left(G_0^{-1}\right)_{ii} =$ total number of points to which the site i is connected, and hence $Tr(G_0^{-1})$ is twice the number of bonds in the network.

Clearly, G_0^{-1} is real and symmetric. As a result, its eigenvalues are real and its eigenbasis complete in the $N-$dimensional space of states. Furthermore, $\det(G_0^{-1}) = 0$. This can be deduced as follows. We first note that since Eq.(2) involves only the phase *differences* (and their time derivatives) it is invariant with respect to the global transformation $\dot{\theta}_i \to \dot{\theta}_i + \dot{\alpha}(\tau)$ $\forall i$. Substituting this into Eq.(4), we have

$$\sum_j \left(G_0^{-1}\right)_{ij}(\dot{\theta}_j + \dot{\alpha}(\tau)) = -d_i = \sum_j \left(G_0^{-1}\right)_{ij}\dot{\theta}_j$$

This implies that $\dot{\alpha}(\tau)\sum_j \left(G_0^{-1}\right)_{ij} = 0$ $\forall i$. I.e., if we fix i and sum over all the columns j, we get zero. (The same is true, of course, if we fix j and sum over i since the matrix is symmetric). Hence $\det(G_0^{-1}) = 0$ and only $(N-1)$ of the N equations in Eq.(2) are independent. (We could, alternatively, note that $(\Psi_0)_i = 1\forall i$ is an eigenvector of G_0^{-1} with eigenvalue 0).

To explicitly evaluate $\dot{\theta}_i$ from θ_i we have to eliminate the extra degree of freedom. For what immediately follows, the most convenient choice is $\sum_i \dot{\theta}_i = 0$. Eq.(4) is then replaced by

$$\sum_j \left(\mathcal{G}_0^{-1}\right)_{ij}\dot{\theta}_j = -D_i \tag{5}$$

where $D_i = d_i$, $i = 1\cdots(N-1)$ and $D_N = 0$ while $\left(\mathcal{G}_0^{-1}\right)_{ij} = \left(G_0^{-1}\right)_{ij}$ $i = 1\cdots(N-1)$, $j = 1\cdots N$ and $\left(\mathcal{G}_0^{-1}\right)_{Nj} = 1\forall j$. Moreover, the vector $[d]$ must satisfy $\sum_i d_i = 0$ as can be seen by performing an additional sum over i in Eq.(4) and using the fact that $\sum_i \left(G_0^{-1}\right)_{ij} = 0$. For JJAs this condition is automatically satisfied since $\dot{\theta}_{ij}$ and $\sin\theta_{ij}$ are odd functions of their arguments and the net external current fed to the array is zero.

One can, in principle, invert $\mathcal{G}_0^{-1}$ and determine $\left[\dot{\theta}\right]$ from $[D]$. This is the usual $\mathcal{O}(N^2)$ process. We shall refrain from adopting this procedure and return, instead, to working with Eq.(2).

In doing so, we shall find it useful to keep in mind some electrostatic analogs of the equations we happen to be dealing with. These emerge clearly if we write the current conservation equation at the site k as

$$I_{k,\mu}^{total} = I_{k,\mu}^s + I_{k,\mu}^n + I_{k,\mu}^{ext} \tag{6}$$

Here $\mu = 1, 2$ represents the x and y directions respectively. Furthermore, $I_{k,\mu}^{total}$, $I_{k,\mu}^s = \sin\Delta_\mu\theta_k$, $I_{k,\mu}^n = \Delta_\mu\dot{\theta}_i$ and $I_{k,\mu}^{ext}$ are the total, superconducting, normal and external currents, respectively, at node k in the μth direction. Using the TCC condition, $\nabla\cdot I_i^{total} = 0$, we have

$$\nabla^2\dot{\theta}_i = \nabla\cdot\left(\vec{I}_i^s + \vec{I}_i^{ext}\right) \tag{7}$$

On comparing Eq.(7) with the Laplace Equation $\nabla^2\phi = -\rho_{total}/\epsilon_0$ and recalling that $\rho_{total} = \rho_{free} + \rho_{bound}$, we arrive at the following correspondences

$$\vec{D}(\vec{r}) \equiv \vec{I}_i^{ext} \tag{8}$$
$$-\vec{P}(\vec{r}) \equiv \vec{I}_i^s \tag{9}$$
$$\phi(\vec{r}) \equiv \dot{\theta}_i \tag{10}$$

Thus the condition imposed above on the $\dot{\theta}_i$ is nothing other than a choice of reference potential or gauge. We, furthermore, note that the JJA thought of as a dielectric medium is highly non–linear. Indeed, $P_{k,\mu} \equiv \sin(-\int E_{k,\mu}dt)$, where $E_{k,\mu} = \Delta_\mu\dot{\theta}_k$ is the μth component of the electric field at site k. This is to be contrasted with $\vec{P}(\vec{r}) \propto \vec{E}(\vec{r})$ for a linear dielectric.

B. The $\mathcal{O}(N\ln N)$ procedure

Going back to Eq.(3), G_0^{-1} can alternatively be inverted by defining the Green's function [see Jackson]

$$\tilde{G}(\vec{r},\vec{r}') = \sum_{\lambda_{\vec{k}}\neq 0} \frac{1}{\lambda_{\vec{k}}}\Psi_{\vec{k}}(\vec{r})\Psi_{\vec{k}}^\dagger(\vec{r}') \tag{11}$$

3

where $\lambda_{\vec{k}}$ are the eigenvalues and $\Psi_{\vec{k}}(\vec{r})$ the orthonormalised eigenvectors of G_0^{-1}, i. e.

$$G_0^{-1}\Psi_{\vec{k}}(\vec{r}) = \lambda_{\vec{k}}\Psi_{\vec{k}}(\vec{r}) \tag{12}$$

and $\vec{r}$ are points on the lattice. More explicitly, the site coordinates $(x_i,\ y_i) \equiv \vec{r}_i$ referred to an origin located at the lower left hand corner of the lattice, are related to the site indices i used earlier by $i = x_i + y_i N_x + 1$. We note that to get a well-defined function, we must explicitly remove from the sum in Eq.(11), the zero mode, which necessarily exists, since G_0^{-1} is singular.

The removal of this mode, however, creates a slight problem. Indeed, if we premultiply by G_0^{-1} and use Eq.(12) we get

$$\sum_{\vec{r}''} G_0^{-1}(\vec{r},\vec{r}'')\tilde{G}(\vec{r}'',\vec{r}) = \sum_{\vec{k}\neq 0} \frac{1}{\lambda_{\vec{k}}}\lambda_{\vec{k}}\Psi_{\vec{k}}(\vec{r})\Psi_{\vec{k}}^{\dagger}(\vec{r}') \tag{13}$$

$$= \sum_{\vec{k}} \Psi_{\vec{k}}(\vec{r})\Psi_{\vec{k}}^{\dagger}(\vec{r}') - \Psi_0(\vec{r})\Psi_0^{\dagger}(\vec{r}')$$

$$= \delta(\vec{r}-\vec{r}') - \frac{1}{\sqrt{L_x L_y}}\begin{pmatrix}1\\\vdots\\1\end{pmatrix}\frac{1}{\sqrt{L_x L_y}}(1,\ 1\cdots 1)$$

which in discretised form is

$$\sum_j \tilde{G}_{ij}\left(G_0^{-1}\right)_{jk} = \delta_{ik} - \frac{1}{L_x L_y} \tag{14}$$

Now if we multiply Eq.(4) from the left by $\tilde{G}$ we get $\dot{\theta}_i - \frac{\sum_i \dot{\theta}_i}{L_x L_y}$ which reads just right, viz.

$$\dot{\theta}_i = \tilde{G}_{ij}d_j \tag{15}$$

provided the $\dot{\theta}_i$ satisfy $\sum_i \dot{\theta}_i = 0$. In other words, with an appropriate gauge choice, $\tilde{G}$ does allow us to invert G_0^{-1}. Indeed, the requirement that it does so fixes the gauge uniquely. It is to be noted that Eq.(15) involves $[d]$ and not $[D]$.

The function, $\tilde{G}(\vec{r},\vec{r}')$, can be easily evaluated for a periodic lattice. The form of the operator $G_0^{-1}(\vec{r},\vec{r}')$, in this case, is given by

$$G_0^{-1}(\vec{r},\vec{r}') = 4\delta_{\vec{r},\vec{r}'} - \delta_{\vec{r}\pm\hat{e}_x,\vec{r}'} - \delta_{\vec{r}\pm\hat{e}_y,\vec{r}'} \tag{16}$$

It is easily checked that the normalised eigenvectors are of the form $\frac{\exp i\vec{k}\cdot\vec{r}}{\sqrt{L_x L_y}}$ and correspond to the eigenvalues

$$\lambda_{\vec{k}} = 4 - 2\cos k_x - 2\cos k_y \tag{17}$$

We note that $\lambda_{\vec{k}=0} = 0$.

Due to the rectangular periodicity of the lattice the eigenvectors must satisfy $\Psi_{\vec{k}}(\vec{r}) = \Psi_{\vec{k}}(\vec{r} + L_i\hat{e}_i) \quad i = x,y$. To fulfil this condition, the wavevectors must in turn be quantised as $k_i = (2n\pi)/L_i \quad i = x,y$ and $n = 0, 1, \cdots (L_{i-1})$. The Green's function of interest is consequently

$$\tilde{G}(\vec{r},\vec{r}') = \frac{1}{L_x L_y}\sum_{\vec{k}\neq 0}\frac{1}{4 - 2\cos k_x - 2\cos k_y}\exp i\vec{k}\cdot(\vec{r}-\vec{r}') \tag{18}$$

We can now estimate the number of steps required to evaluate $\sum_{\vec{r}'}\tilde{G}(\vec{r},\vec{r}')d(\vec{r}')$. The sum over $\vec{r}'$ is a fourier transform and can be carried out in $NlnN$ steps to produce $d(\vec{k})$. Then come the N multiplications $\lambda_{\vec{k}}d(\vec{k})$ followed by the sum over $\vec{k}$, which has the form of an inverse fourier transform, and requires an additional $NlnN$ steps, making a grand total of $N(2lnN + 1)$ multiplications.

Quite generally then, $\dot{\theta}(\vec{r})$ can be evaluated from Eq.(15) by (i) creating an $L_x \times L_y$ matrix $G_0(\vec{k}) = N_{\vec{k}}/\lambda_{\vec{k}}$ where $N_{\vec{k}}$ are the normalisation factors due to $\Psi_{\vec{k}}(\vec{r})$, (ii) evaluating $d(\vec{k}) = \sum_{\vec{r}'} d(\vec{r}')\Psi_{\vec{k}}(\vec{r}')$, this being the forward transform (W), (iii) computing $d'(k) = G_0(\vec{k})d(\vec{k})$, and (iv) taking the 2-D inverse transform $\tilde{W}$ to get $\dot{\theta}(\vec{r}) = \sum_{\vec{k}} d'(\vec{k})\Psi_{\vec{k}}(\vec{r})$. For certain types of transforms and certain values of L_x and L_y, W and $\tilde{W}$ can each be performed by matrix decomposition or row–column techniques with a complexity $\mathcal{O}(N \ln N)$. We now turn to a discussion of this procedure in the context of finite arrays.

C. The Imposition of Boundaries

For a finite array, the general form of G_0^{-1} (Eq.(16)) is modified since now fewer than four bonds meet at all sites on the boundary (see Fig.(1)). For non–corner points on the left edge of the array for example, the operator has the form $3\delta_{\vec{r},\vec{r}'} - \delta_{\vec{r}+\hat{e}_x,\vec{r}'} - \delta_{\vec{r}\pm\hat{e}_y,\vec{r}'}$. However, if Ψ satisfies $\Psi(x_0,y) - \Psi(x_0-1,y) = 0 \quad \forall y$ along this edge, one can continue using the periodic form of G_0^{-1} because then $(4\delta_{\vec{r},\vec{r}'} - \delta_{\vec{r}\pm\hat{e}_x,\vec{r}'} - \delta_{\vec{r}\pm\hat{e}_y,\vec{r}'})\Psi(x_0,y)$ automatically reduces to $(3\delta_{\vec{r},\vec{r}'} - \delta_{\vec{r}+\hat{e}_x,\vec{r}'} - \delta_{\vec{r}\pm\hat{e}_y,\vec{r}'})\Psi(x_0,y)$. We thus see that the finiteness of the array imposes the following boundary conditions on Ψ

$$\Psi(x_0,y) - \Psi(x_0-1,y) = 0 \quad \forall y \tag{19a}$$

$$\Psi(x,y_0) - \Psi(x,y_0-1) = 0 \quad \forall x \tag{19b}$$

$$\Psi(x_L,y) - \Psi(x_L+1,y) = 0 \quad \forall y \quad \text{where} \quad x_L = x_0 + L_x - 1 \tag{19c}$$

$$\Psi(x,y_L) - \Psi(x,y_L+1) = 0 \quad \forall x \quad \text{where} \quad y_L = y_0 + L_y - 1 \tag{19d}$$

where (x_0,y_0) and (x_L,y_L) are the diagonally opposite corners of the rectangular lattice. It is amusing to note that the left–hand side of Eqs.(19a- 19d) are the discrete derivatives of $\Psi(x,y)$ along the edges $x = x_0, y = y_0, x = x_L$ and $y = y_L$, respectively. Thus the finite case poses for us a discretised Neumann boundary value problem.

Furthermore, we note that $\lambda_{\vec{k}}$ (see Eq.(17)) has the symmetries of the square, i.e. $\lambda_{k_x,k_y} = \lambda_{\pm k_x,\mp k_y} = \lambda_{-k_x,-k_y}$. Thus any linear combination of the corresponding eigenvectors,

$$\Psi(x,y) = a_1 \exp i(k_x x + k_y y) + a_2 \exp i(-k_x x + k_y y)$$
$$+a_3 \exp i(k_x x - k_y y) + a_4 \exp i(-k_x x - k_y y) \tag{20}$$

is an eigenvector of G_0^{-1} with the same eigenvalue $\lambda_{\vec{k}}$. To find the specific linear combination, which satisfies the boundary conditions given above, we need merely impose each of Eqs.(19a-19d) in turn. Eq.(19a) can be satisfied by choosing $x_0 = 1/2$, $a_1 = a_2$, $a_3 = a_4$ and the resulting wavefunction is

$$\Psi(x,y) = 2a_1 \cos k_x x \exp(ik_y y) + 2a_3 \cos k_x x \exp(-ik_y y) \tag{21}$$

Subjecting Eq.(21) next to the constraint Eq.(19b), we get

$$\Psi(x,y) = 4a_1 \cos k_x x \cos k_y y \tag{22}$$

where y_0 is now required to be $1/2$ as well. The fact that $x_0 = y_0 = 1/2$ means that the origin of coordinates is chosen on the dual lattice and both coordinates of every lattice point are half integers.

The boundary conditions Eq.(19c) and Eq.(19d) at the right and upper edges of the array can be satisfied by imposing a quantisation condition on $\vec{k}$. Indeed, using Eq.(19c) we have

$$- 8a_1 \cos k_y y \sin(k_x L_x) \sin(\frac{k_x}{2}) = 0 \quad \forall y \tag{23}$$

whereby $k_x = n_x\pi/L_x$, $\quad n_x = 0, 1, \cdots, L_x - 1$. Similarly using Eq.(19d) $k_y = n_y\pi/L_y$, $\quad n_y = 0, 1, \cdots, L_y - 1$.

Thus finally, the orthonormalised wavefunctions we are looking for are

$$\Psi(x,y) = \sqrt{\frac{2}{L_x L_y}} \sqrt{\left(1 - \frac{1}{2}\delta_{k_x,0} - \frac{1}{2}\delta_{k_y,0}\right)} \cos(k_x x) \cos(k_y y) \quad \vec{k} \neq 0 \tag{24}$$

The resulting Green's function to be used in Eq.(11) is thus [9]

$$\tilde{G}(\vec{r},\vec{r}')\frac{4}{L_x L_y} \sum_{\vec{k}\neq 0} \frac{(1 - \frac{1}{2}\delta_{k_x,0} - \frac{1}{2}\delta_{k_y,0})}{4 - 2\cos k_x - 2\cos k_y} \cos(k_x x)\cos(k_y y)\cos(k_x x')\cos(k_y y') \tag{25}$$

The action of this Green's function on a uniform current drive, $I^{ext}(x,y) = I^{ext}(\delta_{x,x_0} - \delta_{x,x_{L_x}})$ can be rigorously shown to be [15]

$$\sum_{y'} \tilde{G}(x,y,x',y')I(x',y') = I(\frac{L_x}{2} - x) \tag{26}$$

III. INCLUSION OF BUS–BARS

Using the techniques of the previous section we generalise the procedure to arrays with either a single or a double busbar (henceforth referred to as SBB and DBB respectively).

In the SBB case, the busbar is normally placed along the current–extraction–edge (see Fig.(2)). The corresponding θ and $\dot{\theta}$ are zero for all time i.e. they do not evolve. The drive edge is however open and can be connected to *any* kind of current profile. Such an array, with a linear profile, has been used previously to study vortex dynamics [12]. On the other hand, an DBB array has shorts along a pair of parallel edges (say those at $x = x_0$ and $x = x_L + 1$ as in Fig(3)). In this case, no current can be injected in the $x-$ direction but the $y-$ direction is available to an arbitrary current drive. Such an array with electrically connected busbars could be used to simulate e.g. the "channel" in the experiments conducted by Van-der-Zant *et al.* [11].

We note that by setting the $\dot{\theta}$ along the busbar to zero and measuring all other $\dot{\theta}$'s with respect to these preassigned variables, we are unambigiously fixing the gauge. Furthermore, since the wavefunction in a rectangular system is separable, i.e. $\Psi(x, y) = \Psi_1(x)\Psi_2(y)$, any change in the boundary conditions along the $x-$ direction, has no impact on $\Psi_2(y)$, which therefore continues to have the form derived in Setion II, viz.

$$\Psi_2(y) = \sqrt{\frac{2}{L_y}}\sqrt{\left(1 - \frac{1}{2}\delta_{k_y,0}\right)}\cos k_y y$$

The altered b.c.s however enter crucially into the determination of $\Psi_1(x)$ and hence in to that of $\Psi(x, y)$.

A. Arrays with a Single Bus-bar

For the SBB case, we have the following b.c.s

$$\Psi_1(x_0) - \Psi_1(x_0 - 1) = 0 \quad \forall y \tag{27a}$$

$$\Psi_1(x_L + 1) = 0 \quad \forall y \quad \text{where} \quad x_L = x_0 + L_x - 1 \tag{27b}$$

The second of these results from the fact that the wavefunction must vanish at the shorted edge as discussed above. Condition Eq.(27a) fixes the form of $\Psi_1(x)$ to be $\sim \cos k_x x$ where x is a half–odd integer, while Eq.(27b) quantises k_x: $k_x = ((2n_x + 1)\pi)/(2L_x + 1)$ $n_x = 0, 1, \cdots, L_x - 1$. The normalisation constant is fixed by the requirement that $A^2 \sum_{p=1}^{L_x} \cos^2 k_x(p - \frac{1}{2}) = 1$. Thus

$$\Psi_1(x) = \sqrt{\left(\frac{2}{L_x + \frac{1}{2}}\right)}\cos k_x x \tag{28}$$

and hence the Green's function $\tilde{G}$ for the case of a single busbar is

$$\tilde{G}(\vec{r}, \vec{r}') = \frac{4}{L_y(L_x + \frac{1}{2})} \sum_{\vec{k}} \frac{(1 - \frac{1}{2}\delta_{k_y,0})}{4 - 2\cos k_x - 2\cos k_y} \cos(k_x x)\cos(k_y y)\cos(k_x x')\cos(k_y y') \tag{29}$$

This $\tilde{G}$ coincides with the G_0 for this case because the zero–mode is absent.

The action of $\tilde{G}$ on a uniform input drive $I^{ext}(x, y) = I^{ext}\delta_{x,x_0}$ can, as in the case of Eq.(26), be exactly shown to be [15]

$$\sum_{y'} \tilde{G}(x, y, x', y')I(x', y') = I(L_x - x + \frac{1}{2}) \tag{30}$$

Although a 1D Fast Cosine transform can be used along the $y-$ axis, this cannot be done for the $x-$direction, since no *fast* Cosine transform of the form

$$C(m) = \sum_{n=0}^{L-1} \tilde{C}(n)\cos\frac{(2n + 1)(2m + 1)\pi}{(4L + 2)}$$

is known to exist [16]. If we resort to usual matrix multiplication along $\hat{e}_x$, the algorithm becomes $\mathcal{O}(2NN_x + 2N \ln N_y + N)$ in complexity and is useful only if $N_y >> N_x$.

A much more efficient approach is to combine the FCT along $\hat{e}_y$ with cylic reduction along the x–direction. This can be carried out as follows [17]. We begin by writing Eq.(4) as

$$\dot{\theta}_{x-1,y} + \dot{\theta}_{x,y'}T_{y',y} + \dot{\theta}_{x+1,y} = -d_{x,y} \tag{31}$$

where the operator $T_{y',y}$ is defined to be $T_{y',y} = \delta_{y',y-1} + \delta_{y',y+1} - 4\delta_{y',y}$ Taking the Cosine transform along the y–direction i. e. setting $\dot{\theta}_{x,y} = \sum_{k_y} \dot{\theta}_{x,k_y} \cos k_y y$, we find that

$$\dot{\theta}_{x,y'}T_{y',y} = \sum_{k_y} 2(\cos k_y - 2)\dot{\theta}_{x,k_y} \cos k_y y \tag{32}$$

As a consequence the y– cosine transform of $\dot{\theta}_{x,y}$ satisfies

$$\dot{\theta}_{x-1,k_y} + \lambda(k_y)\dot{\theta}_{x,k_y} + \dot{\theta}_{x+1,k_y} = -d_{x,k_y} \tag{33}$$

where we have used $\lambda(k_y) = 2(\cos k_y - 2)$. Writing Eq.(33) thrice with x set equal to $x - 1$, x and $x + 1$ respectively, multiplying the second of these equations by $-\lambda(k_y)$ and adding all the three of them together, we get

$$\dot{\theta}_{x-2,k_y} + \lambda^{(1)}(k_y)\dot{\theta}_{x,k_y} + \dot{\theta}_{x+2,k_y} = -d_{x-1,k_y} + \lambda(k_y)d_{x,k_y} - d_{x+1,k_y} = -d^{(1)}_{x,k_y} \tag{34}$$

where $\lambda^{(1)}(k_y) = 2 - (\lambda(k_y))^2$. We note that the x values occurring in Eq.(34) increase in steps of 2 as opposed to 1 in Eq.(33). The two equations are, however, of the same form. We can thus use the reduction procedure repeatedly to get equations with x–values increasing in steps of $4, 8, \cdots$ until after m stages ($2^m = L_x$), we end up with a single equation for the central line of variables:

$$\lambda^{(m-1)}(k_y)\dot{\theta}_{x_0+L_x/2,k_y} = d^{(m-1)}_{x_0+L_x/2,k_y} - \dot{\theta}_{x_0,k_y} - \dot{\theta}_{x_L+1,k_y} \tag{35}$$

The $\lambda^{(p)}(k_y)$ and $d^{(p)}_{x,k_y}$ occurring in these equation are defined by the recursive relations:

$$\lambda^{(p)}(k_y) = 2 - \left(\lambda^{(p-1)}(k_y)\right)^2 \tag{36}$$

$$d^{(p)}_{x,k_y} = d^{(p-1)}_{x-2^{p-1},k_y} - \lambda^{(p-1)}(k_y)d^{(p-1)}_{x,k_y} + d^{(p-1)}_{x+2^{p-1},k_y} \tag{37}$$

Thus, if $\dot{\theta}_{x_0,k_y}$ and $\dot{\theta}_{x_L+1,k_y}$ are known, then $\dot{\theta}_{x_0+L_x/2,k_y}$ can be immediately deduced. The knowledge of $\dot{\theta}_{x_0+L_x/2,k_y}$ leads to that of $\dot{\theta}_{x_0+L_x/4,k_y}$ and $\dot{\theta}_{x_0+3L_x/4,k_y}$ which in turn determine $\dot{\theta}_{x_0+qL_x/8,k_y}$ ($q = 1, 3, 5, 7$) etc. As for the starting values, $\dot{\theta}_{x_L+1,k_y} = 0 \ \forall \ k_y$, since this is the y–cosine transform of $\dot{\theta}_{x,y}$ for $x = x_L + 1$, i.e. taken along the busbar. $\dot{\theta}_{x_0,k_y}$ must however be determined by explicit multiplication. Fortunately, since we know the relevant Green's function explicitly, we can carry this out in $\mathcal{O}(N)$ steps, by taking the cosine transform of Eq.(15):

$$\dot{\theta}_{x_0,k_y} = \frac{4}{L_y(L_x + \frac{1}{2})} \sum_{k_x} \sum_{x'} \frac{\left(1 - \frac{1}{2}\delta_{k_y,0}\right)}{4 - 2\cos k_x - 2\cos k_y} \cos k_x x_0 \cos k_x x' d_{x',k_y} \tag{38}$$

The number of steps required to evaluate all the higher–order divergences $d^{(p)}_{x,k_y}$, $p = 1, \cdots m - 1$ used by the method can be shown to be $N_y \{(N_x/2) - \ln_2 N_x\}$ [15] . With these divergences in hand, the cyclic determination of $\dot{\theta}_{x,k_y}$ has a complexity $\mathcal{O}(N)$. Adding to all this, the number of multiplications involved in carrying out the forward and backward FCTs in the y–direction, we conclude that the entire procedure can be carried out in $\mathcal{O}(2N \ln N_y + 2N + N/2 - N_y \ln_2 N_x)$ steps.

7

B. The Case of a Double Bus-bar

Turning now to the DBB case, we note that the wave-function, $\Psi_1(x)$, must now satisfy the following b.c.s

$$\Psi_1(x_0) = 0 \quad \forall y \tag{39a}$$

$$\Psi_1(x_L + 1) = 0 \quad \forall y \tag{39b}$$

Condition Eq.(39a) fixes the form of $\Psi_1(x)$ to be $\sim \sin k_x x$ where x is an integer while condition Eq.(39b) restricts k_x to the values $(n_x \pi)/(L_x + 1)$, $n_x = 1, \cdots L_x$. The normalisation constant, A, is fixed by $A^2 \sum_{p=1}^{L_x} \sin^2 k_x p = 1$. The resulting orthonormalised wavefunction is then

$$\Psi_1(x) = \sqrt{\frac{2}{L_x + 1}} \sin k_x x \tag{40}$$

and hence $\tilde{G}$ for an array with a double bus–bar is

$$\tilde{G}(\vec{r}, \vec{r}') = \frac{4}{L_y(L_x + 1)} \sum_{\vec{k}} \frac{(1 - \frac{1}{2}\delta_{k_y,0})}{4 - 2\cos k_x - 2\cos k_y} \sin(k_x x) \cos(k_y y) \sin(k_x x') \cos(k_y y') \tag{41}$$

In this case, the transformations along both directions are amenable to fast, i.e. $\mathcal{O}(N \ln N)$, procedures provided $L_x + 1$ and L_y are both integral powers of 2.

IV. DEFECTS

We move on next onto arrays containing defects in the form of broken bonds. As mentioned in Sec. I, arrays of this sort have recently attracted the attention of several groups. Xia and Leath showed that in contrast to networks of resistors [18], where breakdown emanates from the most critical defect, JJAs with missing bonds do not become resistive, the moment any one junction turns critical. Cohn *et al.* [19] showed that defects exert an additional pinning force on a vortex placed in the system. Datta *et al.* [13] demonstrated the existence of multiple vortex sectors in the steady state configurations of the system. They did so by running on large arrays using a modified version of the above algorithm which we now describe in detail.

The evolution equation $\dot{\theta}$ for an array containing a single missing bond between the sites $k \equiv (x_0, y_0)$ and $(k+1) \equiv (x_0 + 1, y_0)$ can be written in matrix notation (see Eq.(2)) as

$$(G_0^{-1} + h)[\dot{\theta}] = [d] \tag{42}$$

where G_0^{-1} is the discrete Laplacian with free, periodic, SBB or DBB boundary conditions and h is given by

$$\begin{aligned} h_{k,k} = h_{k+1,k+1} &= 1 \\ h_{k,k+1} = h_{k+1,k} &= -1 \\ h_{i,j} &= 0 \qquad i, j \neq k, k+1 \end{aligned} \tag{43}$$

Multiplying Eq.(42) with $\tilde{G}$ from the left we get

$$(I + A)[\dot{\theta}] = \tilde{G}[d] = \xi \tag{44}$$

where $A = \tilde{G}h$ and I is the identity matrix. The process of determining $\tilde{G}[d] = \xi$, as already been outlined and can be executed in $N \ln N$ steps. One then needs to evaluate $(1 + A)^{-1}\xi$ efficiently. To this end, we note that A has the form

$$A_{ij} = x_i(\delta_{j,k} - \delta_{j,k+1}) \tag{45}$$

where the numbers x_i are got by explicitly by multiplying G_0 and h. From Eq.(45) it follows that

$$A^q = A(\Delta e)^{q-1} \tag{46}$$

where $\Delta e = x_k - x_{k+1}$. In fact, Δe is the only non-zero eigen value of the matrix A and for the case discussed in Section II C it is given by

$$\Delta e = \frac{4}{L_x L_y} \sum_{\vec{k} \neq 0} \frac{\left(1 - \frac{1}{2}\delta_{k_x,0} - \frac{1}{2}\delta_{k_y,0}\right)}{4 - 2\cos k_x - 2\cos k_y} (\cos(k_x(x_0 + 1)) - \cos(k_x x_0))^2 \cos^2(k_y y_0) \tag{47}$$

where $k_i = (n_i \pi)/L_i$, $n_i = 0 \ldots L_i - 1$ and $i = x, y$. From Eq.(46) it follows that

$$(I + A)^{-1} = I - A + A^2 - A^3 + \cdots = I - \frac{A}{1 + \Delta e} \tag{48}$$

Since the constant matrix $R = -A/(1 + \Delta e)$ contains only two non–zero columns, which are moreover negatives of each other, $[\dot\theta]$ can be determined from ξ in just N multiplicative steps.

The extension of the above procedure to the case of a linear defect [6] consisting of n broken bonds is straight forward as each additional defect introduces into h a 2×2 diagonal block of the form given in Eq.(43). In this case, the series (Eq.(48)) cannot be summed analytically due to the presence of cross terms. An analytic summation is, however, unnecessary. It is sufficient to note that

$$A_{ij} = x_i^1(\delta_{j,k_1} - \delta_{j,k_1+1}) + x_i^2(\delta_{j,k_2} - \delta_{j,k_2+1}) + \cdots x_i^n(\delta_{j,k_n} - \delta_{j,k_n+1}) \tag{49}$$

for bonds missing between k_i and k_{i+1} $(i = 1, 2 \cdots n)$, and that consequently A^q has the same form as above. The numbers x_i^p's occurring in A^q are of course q–dependent. It follows from this that the series can once again be written in the form

$$(I + A)^{-1} = I + R \tag{50}$$

where R is a constant matrix of the form given in Eq.(49). Clearly the action of R on a vector of length N can be determined in nN multiplicative steps. The overall complexity of the algorithm in this case is thus $\mathcal{O}(N \ln N + nN)$. Since the number of broken bonds required to observe various breakdown phenomena [6] is much smaller than N, this results in a very large saving in the time required to perform the computations.

It is interesting to note that the Green's function for the broken bond system G^{bb} satisfies the Dyson's equation [20]

$$G^{bb} = \tilde{G} + \tilde{G}(-h)G^{bb} \tag{51}$$

The matrix $(-h)$ is thus the analog of the potential due to an impurity in an otherwise perfect lattice and the case of the single defect is the analog of the δ function impurity at a given site in the system.

The procedure developed above is for the situation where no pair of broken bonds has any site in common. This ensures that the block matrices introduced in h are always 2×2 rather than $m \times m$, $m > 2$ The general case can be dealt with in a similar manner albeit with an increase in complexity. Lastly, bonds can be added in the interior of the network rather than being eliminated since this does not violate the constraint $\sum_i d_i = 0$.

V. SUMMARY AND DISCUSSION

To summarize, we have extended the Eikman–Himbergen algorithm to a number of practically occurring situations. In particular, we have extended it to the case of a bus–bar placed along one edge of a rectangular array as also to that of electrically connected bus–bars placed along two parallel edges. Finally we have shown that our simulation can be carried out, with only a marginal increase in complexity, for bonds eliminated from or added to the array. In all cases, the open edges can be connected to current sources having any profile whatsoever.

The algorithms for bus–bars as also for perfect arrays subject to magnetic fields, noise, and/or current drives, all involve Green's functions specific to the lattice in question. The Green's function of interest can straightly–forwardly be constructed once the eigen–basis of the corresponding connectivity matrix or discrete Laplacian has been determined. We have shown that this eigen–basis consists precisely of those linear combinations of eigenfunctions of the connectivity matrix for a *periodic* lattice, which satisfy an appropriate set of boundary conditions.

The addition and removal of bonds introduces additional boundaries often in the interior of the array. As a result our earlier procedure becomes invalid. An island of defects created at the center of the array, e.g., defines a lattice version of the sinai billiard problem,which classically has only chaotic solutions. However if the number of bonds eliminated is

small, Green's function techniques which have been extensively used to study disordered solids can be very effectively applied. We have shown that this techniques yields an $\mathcal{O}(N \ln N + nN)$ algorithm. The extensions of such algorithms to the case of 3D arrays is easy since the corresponding eigen–vectors are specified to be either $\exp(i\vec{k} \cdot \vec{r})$ or $\cos(k_x x)$ depending on whether the boundaries are periodic or free boundaries respectively. The eigen–values are now changed to $8 - 2\cos k_x - 2\cos k_y - 2\cos k_z$. In this case, one has to obviously use 3-D transforms.

It is also worth noting that many of the expressions we have derived can be written in terms of continous functions, which are, of course, to be evaluated or sampled only at points belonging to the array. Now if we turn this observation around and think of the discrete lattice as being *produced* by the sampling of the continuous 2–D waveform, we make contact with a long-standing problem in electrical engineering, viz. that of the digitisation and subsequent recovery of band-width limited analog wave-forms. Usually such waveforms are processed as rectangular spaced arrays i. e. they are periodically sampled along the two orthogonally independent variables. However, one can also use hexagonal sampling [21]. Once discretised, the waveforms can be processed as arrays of numbers $x(n_1, n_2)$ by the computer where (n_1, n_2) is a discrete point on which the observable x has some value. The periodicity of the observable $x(n_1, n_2)$ is important as it specifies the eigenfunctions associated with the system. The matrix G_0^{-1} has precisely the information about the chosen sampling raster and the periodicity of the lattice. The raster defines the total number of nearest neighbours of a general site (n_1, n_2) while the periodicity (or finiteness) of the lattice decides the connectivity of the sites at the boundary of the network. The eigenfunctions used in both cases are the same. Indeed, the analogy goes deeper and we can think of the JJA itself as a latticized version of the continuum case (superconducting islands embedded in a normal background much as the Abrikosov lattice consists of normal regions embedded in a superconducting background). Finally, since hexagonally sampled waveforms can be recovered in $\mathcal{O}(N \ln N)$ steps, this analogy opens up the very interesting possibility of working out $\mathcal{O}(N \ln N)$ algorithm for a triangular JJA. This and other related issues are currently under active investigation.

[1] Proceedings of the NATO Advanced Research Workshop on Coherence in Superconducting Networks, Delft, The Netherlands, December 1987, edited by J. E. Mooij and G. B. J. Schon, Physica B **152**, 1-302 (1988).
[2] H. S. J. van der Zant, F. C. Fritschy, T. P. Orlando, and J. E.Mooij, Phys. Rev. Lett. **66**, 2531 (1991).
[3] M. S. Rzchowski, S. P. Benz, M. Tinkham, and C. J. Lobb, Phys. Rev. B **42**, 2041 (1990).
[4] T. S. Tighe, A. T. Johnson, and M. Tinkham, Phy. Rev. B **44**, 10286 (1991).
[5] H. S. J. van der Zant, H. A. Rijken, and J. E. Mooij, J. LowTemp. Phys. **82**, 67 (1991); J. Low Temp. Phys. **79**, 289 (1990).
[6] W. Xia and P. L. Leath, Phys. Rev. Lett. **63**, 1428 (1991); P. L. Leath and W. Xia, Phys. Rev. B **44**, 9619 (1991).
[7] Daniel Dominguez, Phys. Rev. Lett. **72**, 3096 (1994); Daniel Dominguez and Jorge V. José, Phys. Rev. Lett. **69**, 514 (1992).
[8] S. R. Shenoy, J. Phys. C **18**, 5163 (1985); **20**, 2479(E) (1987).
[9] H. Eikmans and J. E. van Himbergen, Phys. Rev. B **41**, 8927 (1990).
[10] Sujay Datta, Shantilal Das, Ravi Mehrotra and Deshdeep Sahdev. (in preparation).
[11] H. S. J. van der Zant, F. C. Fritschy, T. P. Orlando, and J. E.Mooij, Europhys. Lett. **18**, 343 (1992).
[12] R. Mehrotra and S. R. Shenoy, Europhys. Lett. **9**, 11 (1989); Phys. Rev. B **46**, 1088 (1992).
[13] Sujay Datta, Shantilal Das, Ravi Mehrotra and Deshdeep Sahdev. (in communication.).
[14] Ravi Mehrotra, Sujay Datta and Deshdeep Sahdev. (in communication.).
[15] Sujay Datta, Ph.D Thesis, Indian Institute of Technology, Kanpur, India (1995).
[16] K. R. Rao and P. Yip, *Discrete Cosine Transforms, Algorithmns, Advantages, Applications* (Academic Press, Inc., 1990).
[17] W. H. Press, S. A. Teukolsky, W. T. Vetterling and B. P. Flannery, *Numerical Recipes* (Cambridge University Press, Cambridge, 1986).
[18] P. M. Duxbury,P. D. Beale and P. L. Leath, Phys. Rev. Lett. **57**, 1052 (1986), P. M. Duxbury, P. L. Leath, and P. D. Beale, Phys. Rev. B **36**, 367 (1987).
[19] M. B. Cohn, M. S. Rzchowski, S.P. Benz and C. J. Lobb, Phys. Rev. B **43**, 12823 (1991).
[20] John C. Inkson, *Many–Body Theory of Solids* (Plenum, NY, 1984, Chap. 2.).
[21] R. M. Merserau, Proc. of the IEEE **67**, 930, 1979.

Figure Caption

Fig.1 The figure shows the geometry with currents I being injected and extracted at $x = x_0$ and $x = x_{L_x}$ respectively. The • represents the superconducting islands and the line joining them represents a junction.

Fig.2 The figure shows the single bus–bar geometry with currents I being injected $x = x_0$. The short is at $x = x_{L_x+1}$. Note that one can use any current profile in this case.
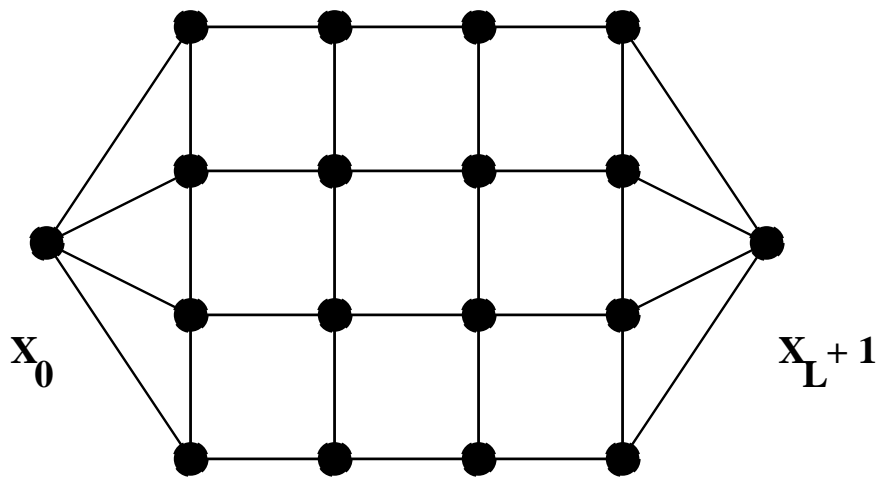
Fig.3 The figure shows the double bus–bar geometry with shorts at $x = x_0$ and $x = x_{L_x+1}$.

$\{ X_{Lx}, Y_{Ly} \}$

I

I

I

I

I

I

I

I

$\{ X_0, Y_0 \}$
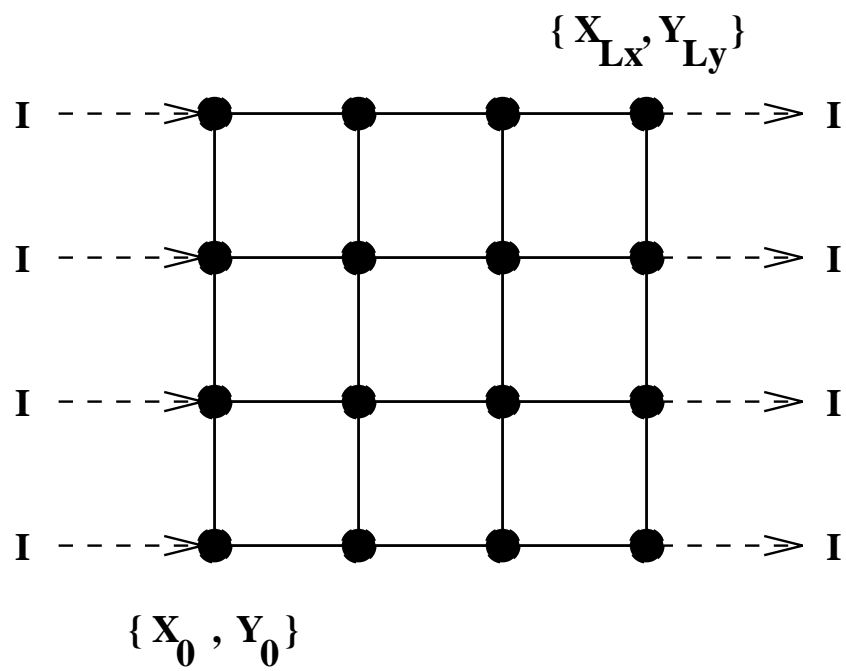
Fig.1 Datta, Das, Sahdev, Mehrotra, Shenoy
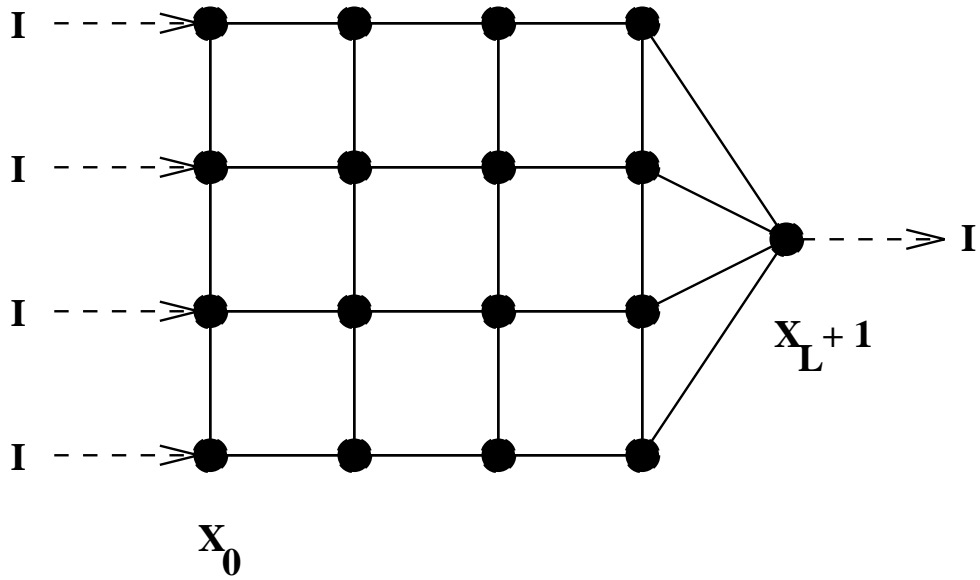
Fig.2 Datta, Das, Sahdev, Mehrotra, Shenoy

X_0

$X_{L}+1$

Fig.3 Datta, Das, Sahdev, Mehrotra, Shenoy